

Fractal Dimension(D_f) Theory of Ismail's Entropy(IE) with Potential D_f Applications to Smart Cities

Ismail A Mageed*

Member IAENG, IEEE, School of Computing, AI, and Electronics, University of Bradford, United Kingdom

*Corresponding Author

Ismail A Mageed, Member IAENG, IEEE, School of Computing, AI, and Electronics, University of Bradford, United Kingdom.

Submitted: 2024, Apr 03; Accepted: 2024, May 27; Published: 2024, Jun 05

Citation: Mageed, I. A. (2024). Fractal Dimension(D_f) Theory of Ismail's Entropy(IE) with Potential D_f Applications to Smart Cities. *J Sen Net Data Comm*, 4(2), 01-10.

Abstract

Ismail entropy (IE), my newly developed entropy measure, is a final generalisation to many generalised entropies found in the literature. This research identifies the fractal dimension of IE. Additionally, this study presents some possible uses of fractal dimension in smart city applications. Concluding thoughts are included at the end of the work along with several difficult outstanding problems and the direction of future research.

Keywords: Fractal Dimension(D_f), Ismail Entropy (IE), Information Theory, Smart Cities

I. Introduction

The Shannonian entropy, $H(X)$ reads [1]:

$$H(X) = \sum_i p(x_i) I(x_i) = -\sum_i p(x_i) \ln(p(x_i)) \quad (1)$$

The probability of the i^{th} event is given by the equation $p(x_i)$. More fundamentally, Ismail entropy reads [2]:

$$H_{(q,U_G)} = \sum_{n=0}^N \varphi((p(n)^q, a_1, a_2, \dots, a_k), k \leq n) \quad (2)$$

φ serves as any well-defined function, $a_1, a_2, \dots, a_k, k \leq n$, serve as any universal parameters, $1 > q > 0.5$.

Notably, the choice of

$$\varphi((p(n)^q, a_1, a_2, \dots, a_k) = \frac{1}{1-q} (p(n)^q - \frac{1}{n})$$

reduces to the Tsallisian Entropy [3] of order q

$$H_T^q(p(n)) = \frac{1}{1-q} (\sum_{n=0}^N (p(n))^q - 1) \quad (3)$$

and $q \rightarrow 1$, H_T^q of (3) reduces to the Shannonian entropic formula (1).

There are several formal mathematical formulations of D_f that can be studied [4-10]. In one such formulation, the scaling factor (ϵ), D_f and the number of sticks (N) needed to cover a shoreline are related through formulae. The following formulas can be used to measure the scaling characteristics and complexity of fractal patterns in spatial dimensions:

$$N \propto \varepsilon^{-D_f} \tag{4}$$

$$\ln N = -D_f = \frac{\ln N}{\ln \varepsilon} \tag{5}$$

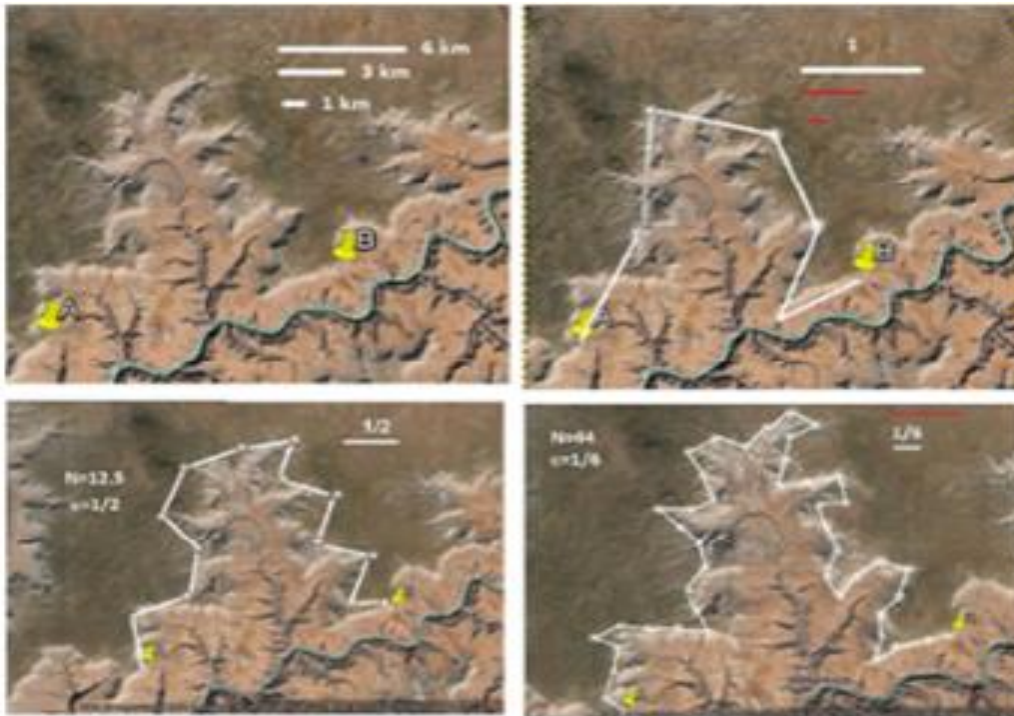


Figure 1: It illustrates how painted portraits were produced using Google Earth satellite images of a portion of the Grand Canyon in Arizona [10].

Impact of N on Scaling Factor

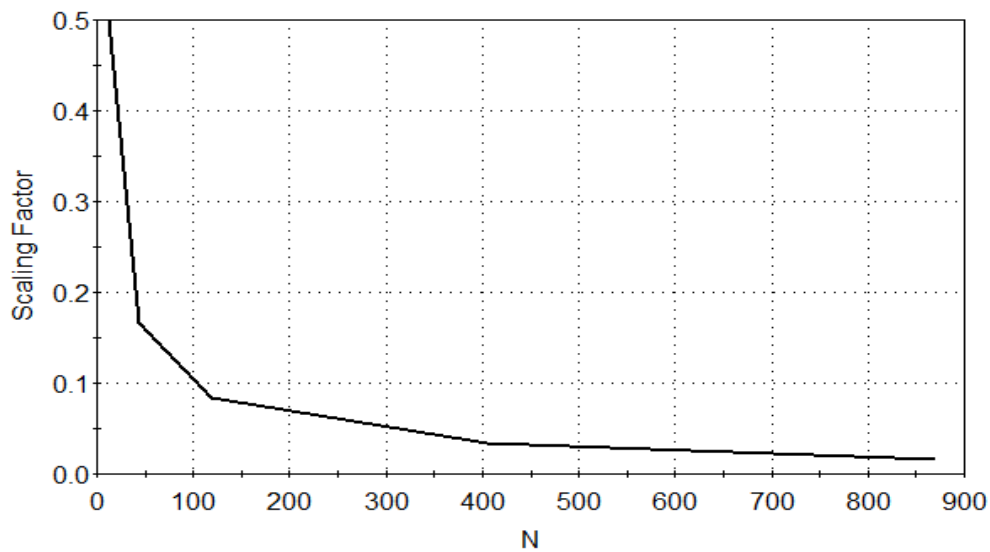


Figure 2

Impact of D_f on ε

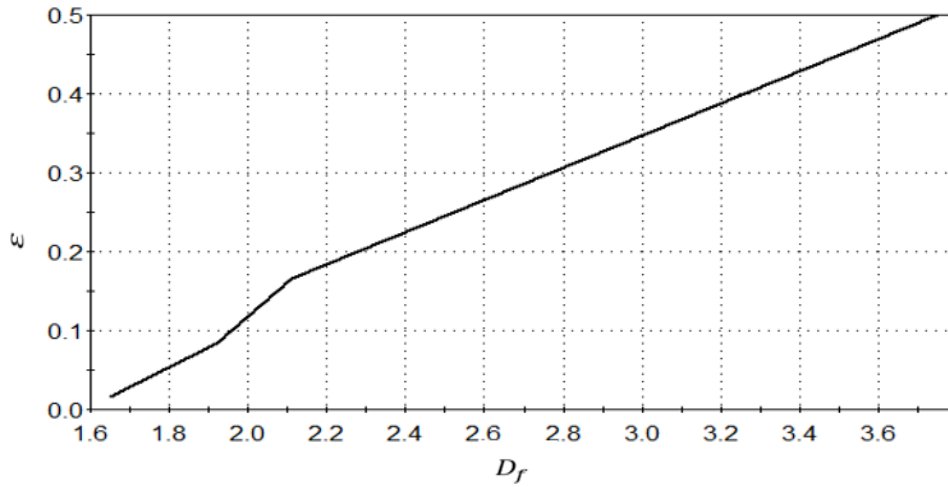


Figure 3

2. Materials and Methods

For occurrences with equal probabilities, that is, $p(i) = 1/N$, an exposition of D_f for Shannon entropy [1], Rényi entropy [3, 11, 12], and Tsallis entropy [13] was conducted in [10].

“Shannonian dimension”, D_s [10] reads:

$$D_s = \lim_{\varepsilon \rightarrow 0} \frac{\ln N}{\ln \frac{1}{\varepsilon}} \quad (6)$$

“Rényian dimension”, D_R [12] reads:

$$D_R = \lim_{\varepsilon \rightarrow 0} \frac{\ln N}{\ln \frac{1}{\varepsilon}} \quad (7)$$

3. Results and Discussion

Theorem 1 D_f (IE) reads:

$$D_f(\text{IE}) = \lim_{\varepsilon \rightarrow 0} \frac{N\varphi(N^{-q}, a_1, a_2, \dots, a_k)}{\ln \frac{1}{\varepsilon}}, \quad k \leq N \quad (8)$$

Proof Engaging (2) and (5), we have

$$D_f(\text{IE}) = \lim_{\varepsilon \rightarrow 0} \frac{\sum_{n=1}^N \varphi\left(\left(\frac{1}{N}\right)^q, a_1, a_2, \dots, a_k\right)}{\ln \frac{1}{\varepsilon}}, \quad k \leq N \quad (9)$$

$$= \lim_{\varepsilon \rightarrow 0} \frac{\sum_{n=1}^N \varphi(N^{-q}, a_1, a_2, \dots, a_k)}{\ln \frac{1}{\varepsilon}} \quad (10)$$

$$= \lim_{\varepsilon \rightarrow 0} \frac{N\varphi(N^{-q}, a_1, a_2, \dots, a_k)}{\ln \frac{1}{\varepsilon}}$$

Engaging (6) and (7), the proof follows.

The following corollary reveals the significance of the findings of Theorem 1.

Corollary 2 D_f (IE) (c.f., (8)) reduces to $D_{Z_{a,b}}$ entropy, namely the fractal dimension of the Generalized Z-Entropy (Gze) [4] given by

$$D_{Z_{a,b}} = \lim_{\varepsilon \rightarrow 0} \frac{1}{(1-q)(a-b)} \frac{(N^{(1-q)a} - N^{(1-q)b})}{\ln \frac{1}{\varepsilon}} \quad (11)$$

Provided that, $1 > q > 0.5, a > 1, b \in \mathbb{R}$ or $b > 0, a \in \mathbb{R}$ with $a \neq b$.

Proof

The choice of

$$\varphi(N^{-q}, a_1, a_2, \dots, a_k) = \frac{1}{(1-q)(a-b)N} [(N^{1-q})^a - (N^{1-q})^b] \tag{12}$$

Such that

$$a_1 = \frac{1}{N(1-q)(a-b)}, a_2 = a_3 = \dots = a_N = 0$$

Following (12), let $N_1 \neq N_2$ such that:

$$\frac{1}{(1-q)(a-b)} [((N_1)^{a(1-q)-1}) - ((N_1)^{b(1-q)-1})] = \frac{1}{(1-q)(a-b)} [((N_2)^{a(1-q)-1}) - ((N_2)^{b(1-q)-1})] \tag{13}$$

By (13), we have

$$[((N_1)^{a(1-q)-1}) - ((N_1)^{b(1-q)-1})] = [((N_2)^{a(1-q)-1}) - ((N_2)^{b(1-q)-1})] \tag{14}$$

(14) reads:

$$[((N_1)^\alpha) - ((N_2)^\alpha)] = [((N_1)^\beta) - ((N_2)^\beta)] \tag{15}$$

Provided that

$$\alpha = a(1-q) - 1, \beta = b(1-q) - 1$$

Engaging mathematical analysis and equation (15),

$$(N_1 - N_2) \left[\begin{matrix} (N_1)^{\alpha-1} + (N_1)^{\alpha-1}N_2 + \dots + (N_2)^{\alpha-1} \\ + (N_1)^{\beta-1} + (N_1)^{\beta-1}N_2 + \dots + (N_2)^{\beta-1} \end{matrix} \right] = 0 \tag{16}$$

Since

$$\left[\begin{matrix} (N_1)^{\alpha-1} + (N_1)^{\alpha-1}N_2 + \dots + (N_2)^{\alpha-1} \\ + (N_1)^{\beta-1} + (N_1)^{\beta-1}N_2 + \dots + (N_2)^{\beta-1} \end{matrix} \right] \neq 0$$

$N_1 = N_2$ (contradiction), which immediately implies the that φ is well defined.

It is implied by (8), (11) and (12), that $D_f(\text{IE})$ reduces to $D_{Z_{a,b}}$.

Corollary 2 is manifested by the fact that $D_{Z_{a,b}}$, the proven special case of $D_f(\text{IE})$, itself reduces to many important D_f 's for many known entropy measures. This is given by the following corollary[4].

Corollary 3 $D_{Z_{a,b}}$ [4] satisfies the following:

- i. $\lim_{a \rightarrow 0, b \rightarrow 0} D_{Z_{a,b}} = D_R$
- ii. $\lim_{q \rightarrow 1} (\lim_{a \rightarrow 0, b \rightarrow 0} D_{Z_{a,b}}) = D_S$
- iii. $\lim_{a \rightarrow 1, b \rightarrow 0} D_{Z_{a,b}} = D_T$
- iv. $\lim_{a \rightarrow k, b \rightarrow -k} D_{Z_{a,b}} = D_{\text{Kaniadakisian entropy}}$
- v. $\lim_{b \rightarrow 0} D_{Z_{a,b}} = D_{\text{Sharma-Mittal entropy}}$

3. D_f Applications to Smart Cities

Local or microscopic chaos and global or macroscopic disorder are the two types of chaos covered by chaos theory [14]. Local chaos is mostly investigated by dissipative structure theory and synergetic theory since it primarily deals with the relationships and interconnections within a system. Chaos theory, on the other hand, focuses specifically on global chaos, which is described as deterministic patterns and behaviors that arise from complex systems.

[14] looked at the growth of smart cities, particularly in China, and stressed how evaluation and planning may suffer from a lack of a basic understanding of smart city systems. Consequently, [14] offered a complete framework for assessing and regulating the

operations of smart cities that considers smart gadgets, ICT, and the dynamics of development. It also implied that the self-organizing system theory could potentially be able to accommodate for the complexity of smart cities.

Smart systems are made up of several interrelated parts, including systems for energy, ICT, economics, security, and institutional culture [14]. As smart city systems are developed, these systems, which are driven by internal institutional culture and ICT mechanisms, evolve from simple smart cell components to more complex entities. Figure 7 demonstrates how these open systems interact with the outside world to exchange information and energy to create a fully self-organizing framework.

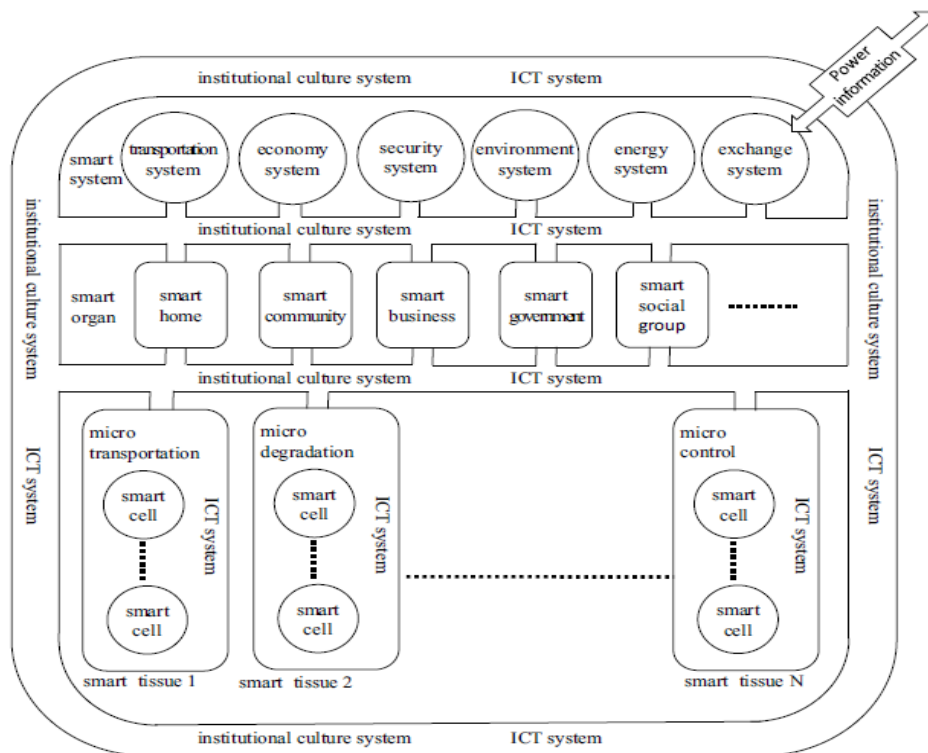


Figure 7: The self-organizing system framework of a smart city refers to the interconnected and interdependent components that make up a smart city, including smart homes, businesses, governments, social groups, and more. These components, known as smart cells, evolve from simple phenomena into complex entities through the influence of institutional culture and information and communication technology (ICT). The framework operates as a self-organizing system, exchanging information and energy with the external world, and follows a hierarchical structure where smart cells form tissues, which form organs, and ultimately form the entire smart city system[14].

An urban road network's overall operation and service level are directly impacted by its structural characteristics [15]. Urban road networks can be analyzed using fractal theory because of their self-similarity and scale invariance. To assess and improve urban road networks, this study calculates and analyses five fractal dimensions of nine districts in Harbin and looks at how they relate

to other variables like area, population, road length, and building density.

Figure 8(c.f., [15]) portrays the map of Harbin, a Chinese city. The main urban area of Harbin has a total of 12,800 roads and the combined length of these roads is 9757.934 kilometers.

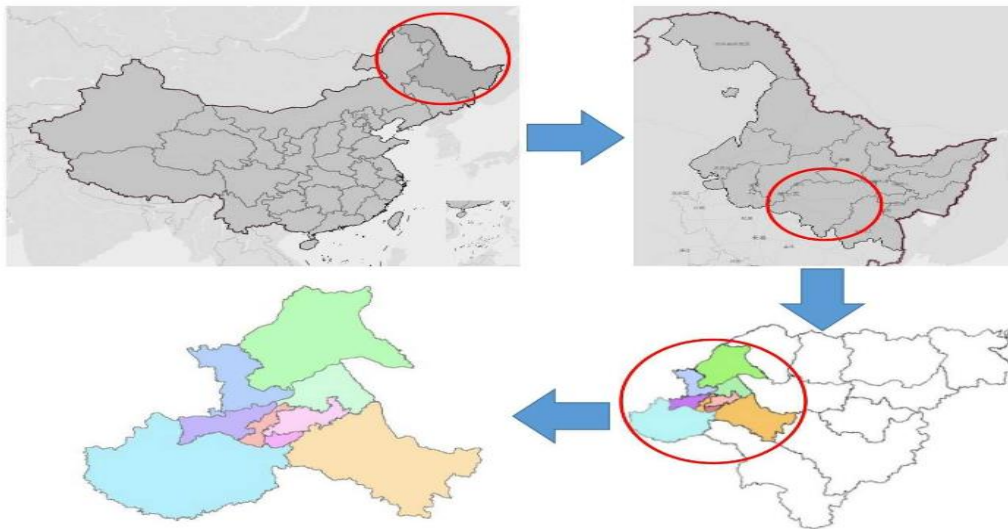


Figure 8

Data including the road network map, area, population, building area, road number, and building number were collected for 9 districts in Harbin, China, to compute the road work's D_f [15]. Shape files were utilized for downloading information about the

metropolitan road network from Open Street Map (OSM). The use of this data to analyze the fractal properties of the Harbin Road network is shown in figure 9.



Figure 9: By examining the data from the road network, it is possible to observe this spatial pattern of road distribution, which has consequences for urban and transportation development in Harbin [15].

In their research, [15] measured five different types of fractal dimensions using images in BMP file format (.bmp). The images in question had a black backdrop with white elements that represented roads and boundaries on them. Figure 10 illustrates

the conversion of nine maps into the appropriate BMP format with varied sizes (width and height) and a resolution of 500 dpi from the GIS software-generated shape file data.

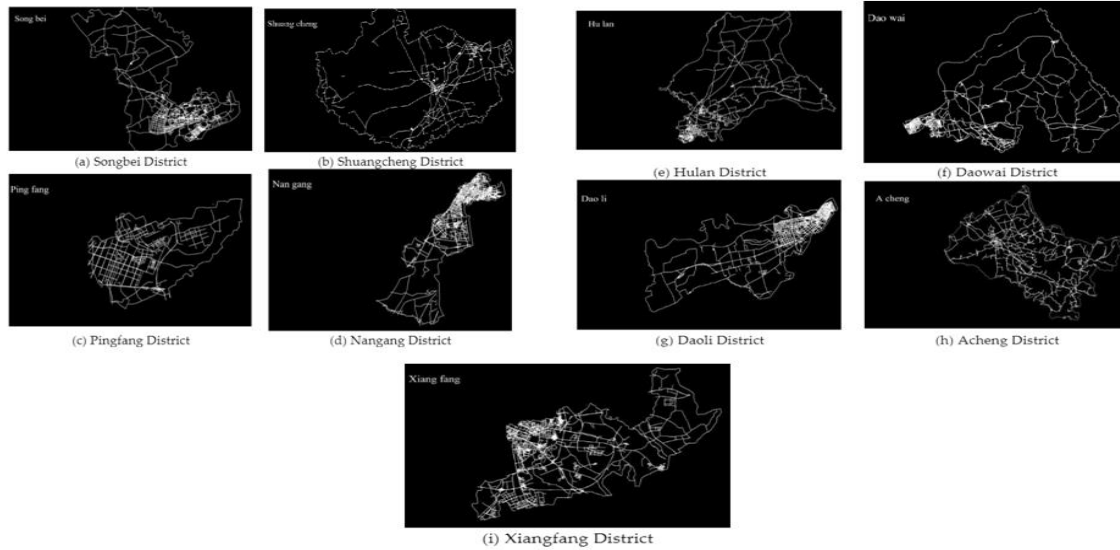


Figure 10 [15].

The urban climate is influenced by various factors and understanding them can help mitigate heat stress in the context of urbanization and climate change [16]. In a study focusing on European cities, it was found that the Urban Heat Island (UHI) phenomenon is influenced by city size, fractality (complexity of urban form), and anisometry (degree of stretching). The study revealed that UHI intensity increases with city size and fractal dimension but decreases with anisometry. Smaller, dispersed, and stretched cities are considered preferable for mitigating UHI, although trade-offs must be made considering the positive effects of large cities. The study focused on the 5,000 largest urban clusters in Europe and analyzed how the UHI intensity is influenced by the size, fractality, and anisometry of the city clusters during the summer months from 2006 to 2013.

- The city size S_C is determined by multiplying the number of cells in a city cluster by the area of each cell. Due to Zipf's law, which states that there are many small cities and few large ones, the logarithm of city $\ln S_C$ is used to reduce the skewness in the data.
- To measure the fractal dimension of city clusters, [16] used the box counting method, which involves counting the number of square boxes needed to cover the structure. Figure 11 (a - c)(c.f., [16]) of the study shows three examples of city clusters with different sizes and levels of fractality, illustrating the concept visually. The box-counting method is used to calculate D_f of city clusters, which provides a measure of their compactness. By analyzing the linear regressions of the log-log scale plots of box-counting results, the slopes of the lines estimate the fractal dimensions, indicating that cities with larger D_f values are generally more compact in shape.
- The anisometry of a city cluster describes how far a city deviates from a circular geometry. It is calculated from the main axis to minor axis ratio of the equivalent ellipse of the city cluster. A higher value of anisometry indicates that the city is more elongated or stretched in shape, as illustrated by the example of Belgrade in Figure 11 (a-c).

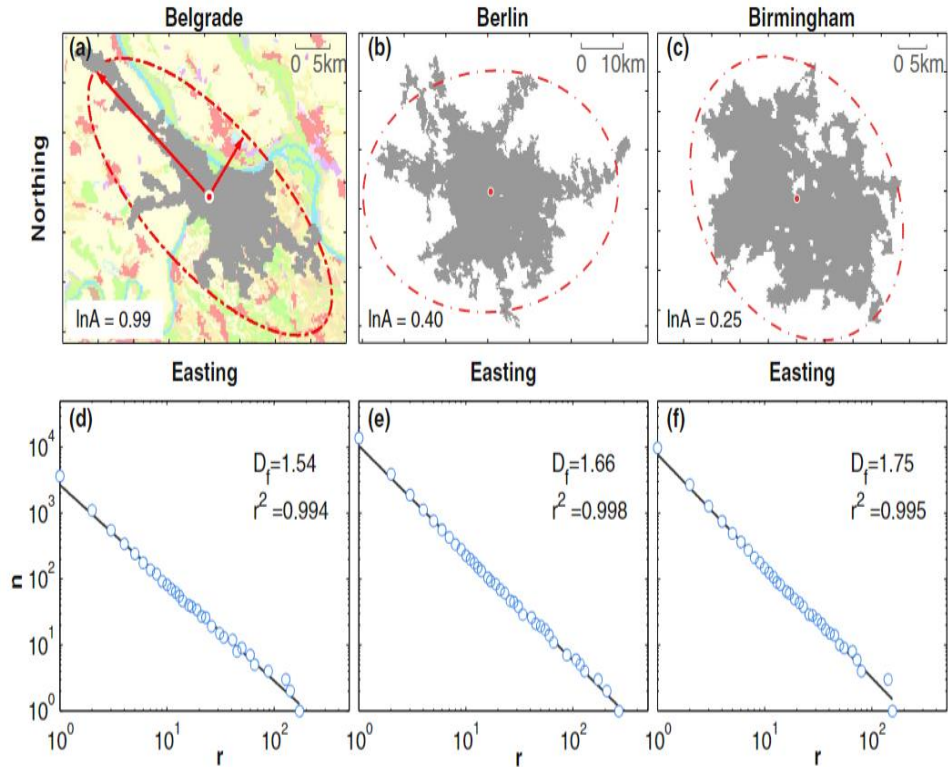


Figure 11

In the context given, scatterplots in figure 12 (c.f., [16]) depict the relationships between the intensity of the midday UHI and three different parameters. Figure 12(a) shows that the UHI intensity rises with city size, with a doubling of city size resulting in an increase in UHI intensity of about 0.4 °C. Moreover, UHI intensity and population size is strongly related [16]. Additionally, quantile regressions reveal heteroscedasticity, indicating stronger

spreading of UHI intensity among large cities. In figure 12(b), the relationship between D_f and UHI intensity is illustrated. The results indicate that as D_f increases, the UHI intensity typically increases by around 2 °C, suggesting that more compact cities tend to have stronger UHI effects. Additionally, in figure 12(c), it is observed that the UHI intensity decreases with increasing anisotropy, with more circular cities exhibiting higher UHI intensities.

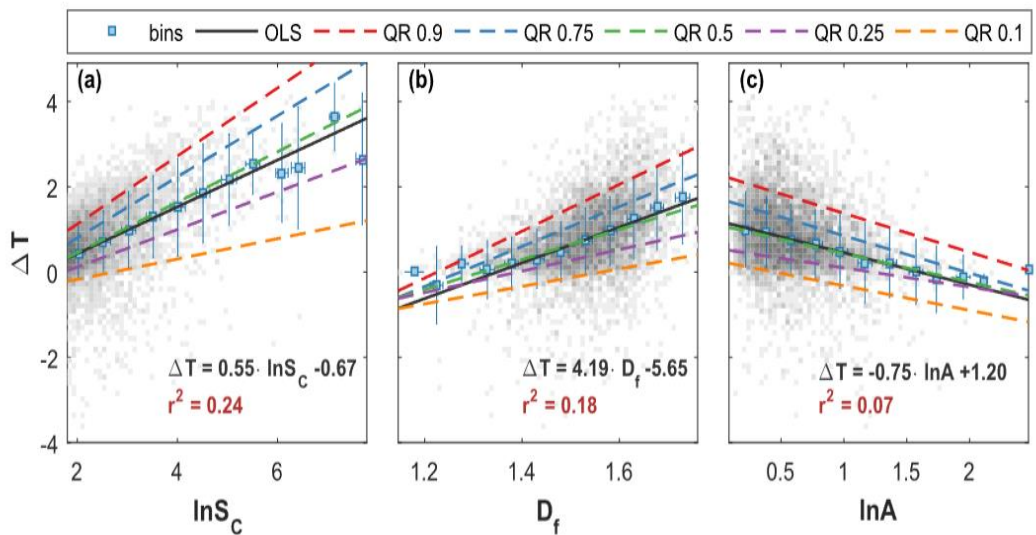


Figure 12: The way Urban Heat Island (UHI) intensity and three factors: logarithm urban cluster size, fractal dimension, and logarithm of anisotropy are related.

The UHI intensity is analyzed using quantile regressions and ordinary least square regression, with the results visualized through linear regressions and quantile regressions. The quantile regressions provide slopes for different quantiles, indicating the varying impact of the factors on UHI intensity [16].

5. Summary

The D_f (IE) is obtained in this exposition. More intriguingly, our research has shown how this finding highlights the dominance of IE, particularly when viewed from the perspective of the fractal dimension. Additionally, various D_f applications to smart city scenarios are discussed.

Now, let's see the proposed research questions:

- **Open Problem One**

Can the mathematical issue of calculating the threshold formalism of the derived fractal dimension of IE be solved regarding all the parameters involved?

- **Open Problem Two**

Can we unlock the threshold of both fractal dimensions, particularly for the long-range interactions descriptor (q) to capture the missing link between statistical physics, randomness, thermodynamics, and fractal geometry as we get closer to the IE's Snow Koch flake fractal dimension ($N = 4$ and $\varepsilon = \frac{1}{3}$) and the Sierpinski Gasket ($= 3$ and $\varepsilon = \frac{1}{2}$)?

- **Open Problem Three**

Talking short- range interaction, in correspondence to q ($q \notin (0.5,1)$), what will be the solution for both open problems One and Two if it is solvable?

- **Open Problem Four**

Is it possible to have negative values for the obtained fractal dimension of IE? If yes, then what are the physical interpretations for this case.

- **Open Problem Five**

If open Problem Four is unlocked, can we solve this sophisticated open problem to get the corresponding value of q ?

- **Open Problem Six**

Is the open problem of determining the threshold parametric patterns for the undertaken generated Snow Kochflake and Sierpinski Gasket dimensions of Ismail's Second, fourth and the current entropies solvable? If yes, then how could we fine tune the discovered regions of increasability and decreasability [17].

The frontiers are open for unlimited explorations. The next phase of research includes answering the above open research problems and exploring more new avenues of D_f applications to other scientific and other interdisciplinary themes of research will be

addressed [18].

References

1. Mageed, I. A., & Zhang, Q. (2022, September). An Introductory Survey of Entropy Applications to Information Theory, Queuing Theory, Engineering, Computer Science, and Statistical Mechanics. In *2022 27th International Conference on Automation and Computing (ICAC)* (pp. 1-6). IEEE.
2. Mageed, I. A., & Zhang, Q. (2022, October). An Information Theoretic Unified Global Theory For a Stable $M/G/1$ Queue With Potential Maximum Entropy Applications to Energy Works. In *2022 Global Energy Conference (GEC)* (pp. 300-305). IEEE.
3. Kouvatso, D. D., Mageed, I. A., Anisimov, V., & Limnios, N. (2021). Non-Extensive Maximum Entropy Formalisms and Inductive Inferences of Stable $M/G/1$ Queue with Heavy Tails. *Advanced Trends in Queueing Theory*, 2.
4. Mageed, I. A., & Bhat, A. H. (2022). Generalized Z-Entropy (Gze) and Fractal Dimensions. *Appl. Math*, 16(5), 829-834.
5. Zhou, L., Johnson, C. R., & Weiskopf, D. (2020). Data-driven space-filling curves. *IEEE transactions on visualization and computer graphics*, 27(2), 1591-1600.
6. Wang, W. J., Xu, X., Shao, Y., Liao, J. W., Jian, H. X., Xue, B., & Yang, S. G. (2022). Fractal growth of giant amphiphiles in langmuir-blodgett films. *Chinese Journal of Polymer Science*, 40(6), 556-566.
7. Sadem, Z., Fathi, B., & Mustapha, L. (2023). Image edge detection and fractional calculation. *International Journal of Advanced Natural Sciences and Engineering Researches*, 7(7), 222-225.
8. Nayak, S. R., & Mishra, J. (2023). Analysis of medical images using fractal geometry. In *Research Anthology on Improving Medical Imaging Techniques for Analysis and Intervention* (pp. 1547-1562). IGI Global.
9. Gao, X. L., Shao, Y. H., Yang, Y. H., & Zhou, W. X. (2022). Do the global grain spot markets exhibit multifractal nature?. *Chaos, Solitons & Fractals*, 164, 112663.
10. Zhao, T., Li, Z., & Deng, Y. (2023). Information fractal dimension of random permutation set. *Chaos, Solitons & Fractals*, 174, 113883.
11. Pons, F., Messori, G., & Faranda, D. (2023). Statistical performance of local attractor dimension estimators in non-Axiom A dynamical systems. *Chaos: An Interdisciplinary Journal of Nonlinear Science*, 33(7).
12. Mageed, I. A., & Zhang, Q. (2023). The Rényiian-Tsallisian Formalisms of the Stable $M/G/1$ Queue with Heavy Tails Entropian Threshold Theorems for the Squared Coefficient of Variation. *electronic Journal of Computer Science and Information Technology*, 9(1), 7-14.
13. Mageed, I. A., & Zhang, Q. (2022, September). Inductive Inferences of Z-Entropy Formalism (ZEF) Stable $M/G/1$ Queue with Heavy Tails. In *2022 27th International Conference on Automation and Computing (ICAC)* (pp. 1-6). IEEE.
14. Yan, J., Liu, J., & Tseng, F. M. (2020). An evaluation system

-
- based on the self-organizing system framework of smart cities: A case study of smart transportation systems in China. *Technological Forecasting and Social Change*, 153, 119371.
15. Deng, H., Wen, W., & Zhang, W. (2023). Analysis of Road Networks Features of Urban Municipal District Based on Fractal Dimension. *ISPRS International Journal of Geo-Information*, 12(5), 188.
 16. Liu, B., Guo, X., & Jiang, J. (2023). How Urban Morphology Relates to the Urban Heat Island Effect: A Multi-Indicator Study. *Sustainability*, 15(14), 10787.
 17. Mageed, I. A. (2023, November). Fractal Dimension (D f) Theory of Ismail's Second Entropy (H_q) with Potential Fractal Applications to ChatGPT, Distributed Ledger Technologies (DLTs) and Image Processing (IP). In *2023 International Conference on Computer and Applications (ICCA)* (pp. 1-6). IEEE.
 18. Mageed, I. A. (2023, November). Fractal Dimension (D f) of Ismail's Fourth Entropy ($H_{IV}(q, a_1, a_2, \dots, a_k)$) with Fractal Applications to Algorithms, Haptics, and Transportation. In *2023 International Conference on Computer and Applications (ICCA)* (pp. 1-6). IEEE.

Copyright: ©2024 Ismail A Mageed. This is an open-access article distributed under the terms of the Creative Commons Attribution License, which permits unrestricted use, distribution, and reproduction in any medium, provided the original author and source are credited.